PROTEIN STRUCTURE REPORT

Solution structure of the human HSPC280 protein

Jinzhong Lin, Tao Zhou, and Jinfeng Wang*

National Laboratory of Biomacromolecules, Institute of Biophysics, Chinese Academy of Sciences, Beijing 100101, China

Received 27 August 2010; Accepted 1 November 2010
DOI: 10.1002/pro.548
Published online 16 November 2010 proteinscience.org

Abstract: The human HSPC280 protein belongs to a new family of low molecular weight proteins, which is only present in eukaryotes, and is absent in fungi. The solution structure of HSPC280 was determined using multidimensional NMR spectroscopy. The overall structure consists of three α-helices and four antiparallel β-strands and has a winged helix-like fold. However, HEPC280 is not a typical DNA-binding winged helix protein in that it lacks DNA-binding activity. Unlike most winged-helix proteins, HSPC280 has an unusually long 13-residue (P62–V74) wing 1 loop connecting the β3 and β4 strands of the protein. Molecules of HSPC280 have a positively charged surface on one side and a negatively charged surface on the other side of the protein structure. Comparisons with the C-terminal 80-residue domain of proteins in the Abra family reveal a conserved hydrophobic groove in the HSPC280 family, which may allow HSPC280 to interact with other proteins.

Keywords: human HSPC280; winged helix-like protein; positively charged surface; negatively charged surface; hydrophobic groove

Introduction

The human HSPC280 protein is encoded by the C6ORF115 gene, which was first cloned from human fetal liver and CD34+ stem cells. There are two possible ORFs in the gene: one gives a protein of 134 amino acids, whereas the other codes for a smaller protein of 81 amino acids. Several proteomic studies have confirmed that HSPC280 is a small protein of 81 amino acids *in vivo* and that its first methionine residue is acetylated.[1]

There is no functional or structural information available for HSPC280. However, HSPC280 is readily detected by proteomic analyses in human tissues or cells such as plasma,[1–3] intestinal epithelial cells,[4] chondrocytes,[5] platelets,[6] and liver.[7] In addition to its detection at the protein level, EST and gene expression profiling[8,9] suggest that HSPC280 is also expressed in other tissues. Moreover, HSPC280 seems to be an abundant protein *in vivo*. In platelets, for example, HSPC280 is ranked 37 in the top 50 most abundant proteins.[10] Its wide expression and high abundance suggest that HSPC280 might play an important role in cellular processes. C6ORF115 is downregulated in diffuse-type gastric cancer.[11] In breast cancer cells, the C6ORF115 gene is upregulated after treatment with DHC, a cannabinoid which has antiproliferative effects.[12] In a study

Additional Supporting Information may be found in the online version of this article.

Grant sponsor: Knowledge Innovation Project of the CAS; Grant number: KSCX1-SW-17; Grant sponsor: National Natural Science Foundation of China; Grant number: NNSFC 30770434.

*Correspondence to: Jinfeng Wang, National Laboratory of Biomacromolecules, Institute of Biophysics, Chinese Academy of Sciences, Beijing 100101, China. E-mail: jfw@sun5.ibp.ac.cn

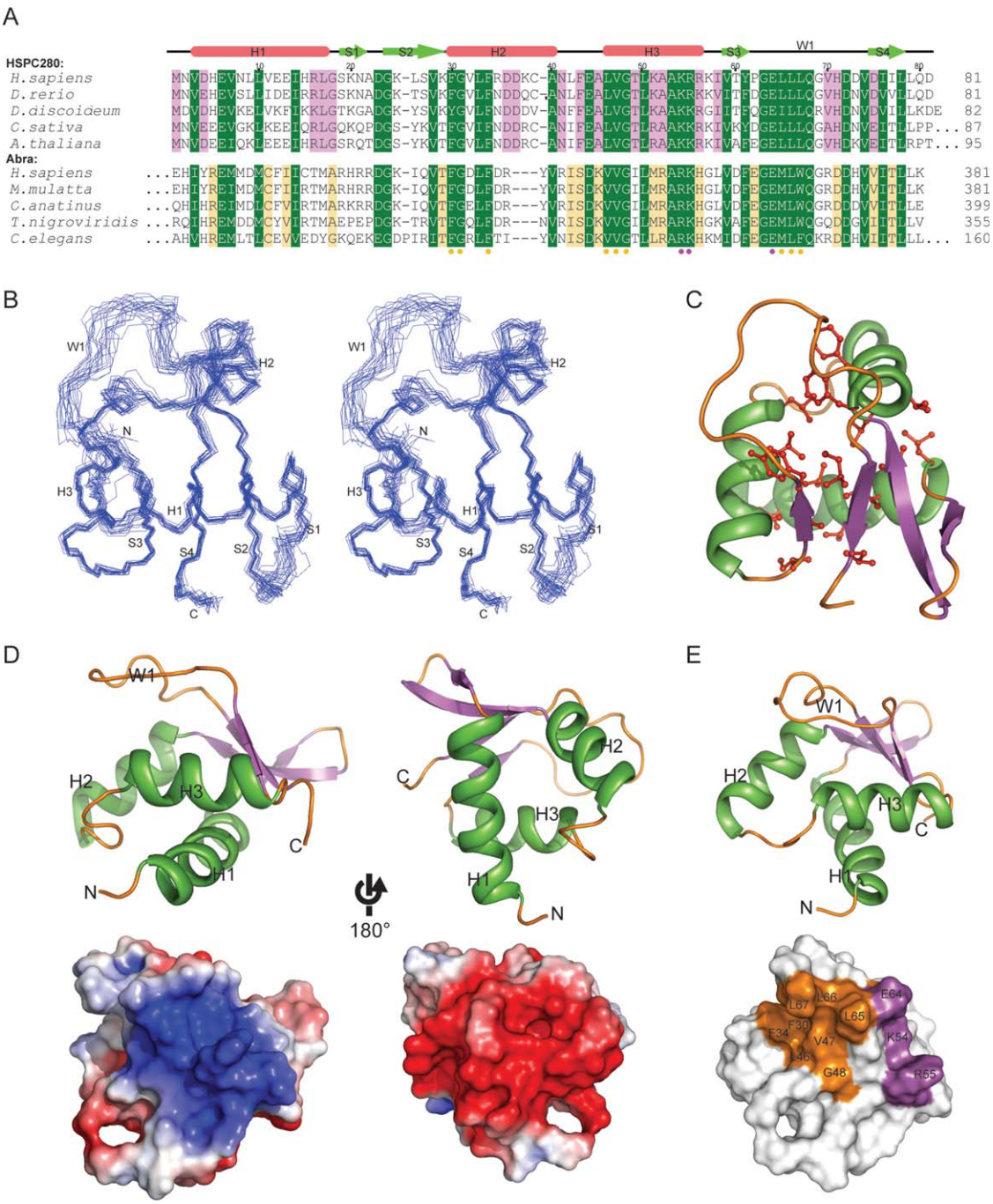

Figure 1. A: Multiple sequence alignment of proteins from the HSPC280 and Abra families. The alignment was generated by MAFFT and edited manually. The sequence length for each protein is shown. Conserved residues in both families are shaded in green. Residues conserved in individual families are shaded in purple for HSPC280 and yellow for Abra, respectively. Secondary structural elements (letter "H" stands for α-helix, whereas "S" for β-strand) are indicated according to the HSPC280 structure determined here. Residues forming conserved hydrophobic and hydrophilic patches on the protein surface are marked by solid yellow and solid purple circles, respectively. B: A stereo-view of the superimposition of the 20 lowest-energy structures. C: Hydrophobic interactions in HSPC280. The protein orientation is the same as in (B). D: Electrostatic surface of HSPC280 calculated with Adaptive Poisson-Boltzmann Solver. In the lower panel, positively and negatively charged surfaces are colored blue and red, respectively. In the upper panel, the ribbon diagrams indicate the respective protein orientations. Contour levels are set to −3.0 kT/e (red) and +3.0 kT/e (blue). E: Hydrophobic and hydrophilic surface patches conserved between HSPC280 and the Abra family. The conserved hydrophobic and hydrophilic surfaces are colored in orange and purple, respectively, in the HSPC280 structure. Residues contributing to these surface patches are labeled. The protein is in a similar orientation as that in (D), left panel.

of the early gene expression profile during spinal cord regeneration in the salamander, C6ORF115 was upregulated from Day 5 after tail amputation along with many other genes associated with cell cycle regulation, suggesting that the HSPC280 protein may play a role in cell proliferation.

A blast search using the HSPC280 sequence revealed that HSPC280 belongs to a new family of low molecular weight proteins which exists only in eukaryotes but is not present in fungi. The sequences of HSPC280 are highly conserved among different species [Fig. 1(A)]. Here, we report the solution structure of human HSPC280 showing that HSPC280 has a winged helix-like fold with an unusually long wing 1 and a very short wing 2. Three α-helices form a globular, three-helix cluster, which is packed against an antiparallel four-stranded β-sheet. NMR-titration with DNA and (electrophoretic mobility shift assay) EMSA experiments demonstrated that HSPC280 is not a typical winged-helix protein. Nevertheless, the conserved hydrophobic groove on the protein surface of the HSPC280 family may confer HSPC280 with physiological functions different from other winged-helix proteins.

Results and Discussion

The structure of HSPC280 adopts a winged helix fold

The structure of HSPC280 was determined in aqueous solution at pH 4.4 using a hetero-nuclear multidimensional NMR method. The protein construct encompasses 81 residues and has a His-tag stretch of eight residues at the C-terminus. Backbone resonance assignments were obtained for nearly all residues, with the exception of one proline and five residues in two loop regions, which showed no resonance signals in the 2D ^{1}H-^{15}N HSQC spectrum (Supporting Information, Fig. S1). A superposition of the 20 lowest energy HSPC280 structures is shown in Figure 1(B) and illustrates a well-determined winged helix-like fold. PROCHECK-NMR analysis indicated that the NMR structures of HSPC280 have a good backbone conformational regularity for 89.4% of all residues in the most favored regions. The detailed structure statistics and PROCHECK-NMR analysis are given in Table I.

The overall structure of HSPC280 comprises three α-helices (α1:V3-L17, α2:F30-A40, and α3:L46-R56) and four β-strands (β1:G18-K20, β2:G24-K29, β3:V59-Y61, and β4:D75-L78) in the canonical order α1-β1-β2-α2-α3-β3-β4. Strands β2 and β3 are antiparallel to β1 and β4 forming an antiparallel 4-stranded β-sheet (β1↑, β2↓, β4↑, β3↓), and helices α1, α2, and α3 construct a three-helix cluster [Fig. 1(B)]. A five-residue loop (N41-A45) links helices α2 and α3 ($L_{\alpha2\alpha3}$) while K57 and I58 link helix α3 to strand β3 ($L_{\alpha3\beta3}$). Residues V7, L10, V11, I14, and L17 from helix α1, residues F30, G31, V32, L33, and F34 from helix α2, and residues L46, L50, A52, and A53 from helix α3 in the three-helix cluster are engaged in hydrophobic interactions with residue V28 in strand β2, residues V59 and Y61 in strand β3, and residues I76 and L78 in strand β4 and residue I58 in $L_{\alpha3\beta3}$ [Fig. 1(C)]. The hydrophobic interactions should generate stable packing of the three α-helices against the antiparallel β-strands β2, β3, and β4. A 13-residue loop (P62–V74) between strands β3 and β4 is referred to as the first wing (wing 1), whereas the three C-terminal residues after strand β4 are referred to as the second wing (wing 2). Five salt-bridges were identified between different secondary structural elements using distance cutoffs of ≤4.0 Å. They are K29NZ-D75OD between strands β2 and β4, D4OD-R56NH between helices α2 and α3, K54NZ-E64OE and K51NZ-E64OE between helix α3 and the N-terminal of wing 1, and K29NZ-D73OD between strand β2 and the C-terminal of wing 1. Unlike most winged-helix proteins, HSPC280 has an unusually long wing 1 similar to that in the winged-helix domains of HSF[13,14] and TFE/TFIIA,[15] and a very short wing 2. Because the primary sequence of HSPC280 has very little similarity to any known

Table I. *Distance and Dihedral Angle Restraints Used for Structure Calculations and Structural Statistics for the Family of the 20 Lowest Energy Structures of HSPC280*

Structural statistics for the final structures of HSPC280	
Number of distance restraints	
Total NOEs	1301
Intraresidual NOEs ($\|i-j\|=0$)	349
Sequential NOEs ($\|i-j\|=1$)	329
Medium-range NOEs ($\|i-j\|=2$–4)	245
Long-range NOEs ($\|i-j\|=5$)	378
Hydrogen bonds	64
Dihedral angle restraints	
Phi and Psi angles	137
RMSD from idealized covalent geometry	
Bonds (Å)	0.0034 ± 0.0002
Angles (°)	0.48 ± 0.03
Impropers	1.39 ± 0.30
CNS Energies (kcal/mol)	
E_{Overall}	−3534.4 ± 67.9
E_{Bonds}	16.2 ± 1.3
E_{Angles}	89.7 ± 6.1
E_{Improp}	50.7 ± 7.6
E_{Dihe}	417 ± 7.2
E_{Vdw}	−333.6 ± 12.5
E_{Elec}	−3795.3 ± 68.1
E_{NOE}	17.8 ± 4.3
E_{Cdih}	2.6 ± 0.8
Number of restraint violations	
Distance restraint violations >0.2 Å	0
Dihedral angle restraints >5°	0
PROCHECK_NMR Ramachandran map analysis	
Most favored regions	89.4%
Additional allowed regions	9.7%
Generously allowed regions	0.3%
Disallowed regions	0.5%
Average pair-wise RMSD	
Secondary (3–21, 24–40, 46–61, 75–78)	
Backbone, 2nd struct	0.63 ± 0.09
Heavy atoms, 2nd struct	1.36 ± 0.13
Global	
Backbone, all residues	1.15 ± 0.20
Heavy atoms, all residues	2.00 ± 0.24

winged-helix proteins or domains, it is possible that HSPC280 represents a new class of winged-helix proteins.

The HSPC280 molecule has a unique electrostatic surface. The basic residues K51-X-X-K54-R55-R56 at the C-terminal of helix α3, together with K57 in loop $L_{\alpha3\beta3}$, form a positively-charged surface on one side of the protein [lower left panel of Fig. 1(D)]. The acidic residues, D4, E6, E12, and E13 from helix α1, D36 from helix α2, and E44 in loop $L_{\alpha2\alpha3}$ are distributed on the opposite side of HSPC280, forming a negatively charged surface [lower right panel of Fig. 1(D)], rendering HSPC280 a mildly acidic protein with a theoretical isoelectric point (Ip) of 5.8. The charge characteristics of the protein surface may attribute HSPC280 with a physiological function that is different from other winged-helix proteins.

To determine whether the HSPC280 structure is similar to that of known winged-helix structures, we submitted the HSPC280 atomic coordinates to the DALI server.[16] Structure-based homology analysis with DALI revealed hundreds of proteins or domains having winged-helix folds with *Z*-scores larger than 4.0. Among them, a putative transcriptional regulator protein from *Pseudomonas aeruginosa* (PDB code: 2HR3) had the highest DALI score (7.4) and an rmsd of 2.3 Å over 64 C_α atoms. Many of the other most closely related structures are transcriptional regulators from the MarR family involved in the development of antibiotic resistance (PDB codes: 2HR3, 3BPV, 2PFB, and 3ECO). The key structural feature of MarR-type proteins is that they are dimeric because of the interaction of the additional helices which flank the winged-helix DNA-binding core.[17]

The sequence of HSPC280 shows little identity with other winged-helix proteins revealed by DALI analysis despite their resemblance in structure [Fig. 2(A)]. Structure-based alignment of their sequences showed that only the hydrophobic residues inside the structural core of the winged-helix fold are conserved, whereas the residues on the protein surface vary significantly [Fig. 2(A,B)]. Because HSPC280 most closely resembles proteins from the MarR family, we compared the structure of HSPC280 with OhrR, a member of the MarR family, which interacts with DNA (PDB code: 1Z9C). The rmsd between these two proteins is 2.9 Å over 63 C_α atoms. OhrR binds DNA through its recognition helix at the major groove and its basic wing at the minor groove. Almost all the residues of OhrR involved in its contact with DNA are absent in HSPC280 [Fig. 2(A,C)], suggesting that HSPC280, unlike other winged-helix proteins from the MarR family, is unlikely to bind DNA.

HSPC280 is not a typical winged-helix protein

The winged-helix fold is very often found in transcription factors and is responsible for binding with specific DNA sequences. DNA-binding winged-helix proteins often interact with DNA by insertion of helix α3, also called the "recognition helix," into the major groove of DNA, and through contact between one or both of the wings of the protein and the ribose-phosphate backbone and/or minor groove of DNA. Typical examples of such proteins are HNF-3γ,[18] the E2F-4 fragment,[19] and genesis.[20] Their DNA binding sites are continuous positively charged surfaces due to the basic residues on helix α3 and the wings. In the case of FREAC-11 (forkhead related activator 11), also known as S12,[21] DNA binding occurs mainly by insertion of helix α3 into the major groove of the DNA, along with the interaction of wing 2 with the ribose-phosphate backbone. In contrast, the face of helix α3 of the eukaryotic transcription factor RFX1[22] is neutral, and a cluster of the basic residues is present on wing 1. Wing 1 of RFX1 binds to the major groove of DNA, while only one side-chain of the helix α3 has contact with the minor groove of DNA. Moreover, sequence stretches of the loop preceding helix α3 and wing 1, showing high internal mobility, have been shown to be important for DNA recognition/interaction in forkhead transcription factors.[23–25] In the structure of HSPC280, the basic residues K51-X-X-K54-R55-R56 of helix α3 together with K57 in loop $L_{\alpha3\beta3}$ form a continuous positively charged surface [left panel of Fig. 1(D)] which is ideal for association with the negatively charged phosphodiester backbone of DNA. In addition, ^{1}H-^{15}N steady-state NOE and ^{15}N R_2 and R_1 measurements indicate a very flexible wing 1 and the possible conformational exchange motion of loop $L_{\alpha2\alpha3}$ which precedes helix α3 (Supporting Information Fig. S2). This was also reflected by very weak or unobservable amide signals for residues F43-E44-A45-L46 from loop $L_{\alpha2\alpha3}$ preceding helix 3 and residues L66–L67, G69, and H71 from wing 1 in the 2D ^{1}H-^{15}N HSQC spectrum of HSPC280 (Supporting Information Fig. S1). In addition, the structure determined for HSPC280 also showed a lack of backbone coordinate precision in these two structural regions [Fig. 1(B)]. In line with these structural similarities to nucleic acid-interacting proteins, it is possible that HSPC280 interacts with nucleic acids. However, unlike typical winged-helix proteins, wing 1 of HSPC280 carries three negatively charged (E64, D72, and D73) but only one positively (H71) charged residue. Moreover, the groove between helix α3, wing 1 and helix α2, which accommodates the DNA backbone in typical DNA-binding winged-helix proteins, is hydrophobic in nature. Hydrophobic sidechains of residues F30 and F34 from helix α2; L46, V47, G48, L50 from helix α3; and G63, L65, L66, and L67 from wing 1 provide most of the hydrophobicity of this groove in HSPC280. These structural properties make it unlikely that HSPC280 binds DNA like a typical DNA-binding winged helix protein, despite some features that seem to suggest this.

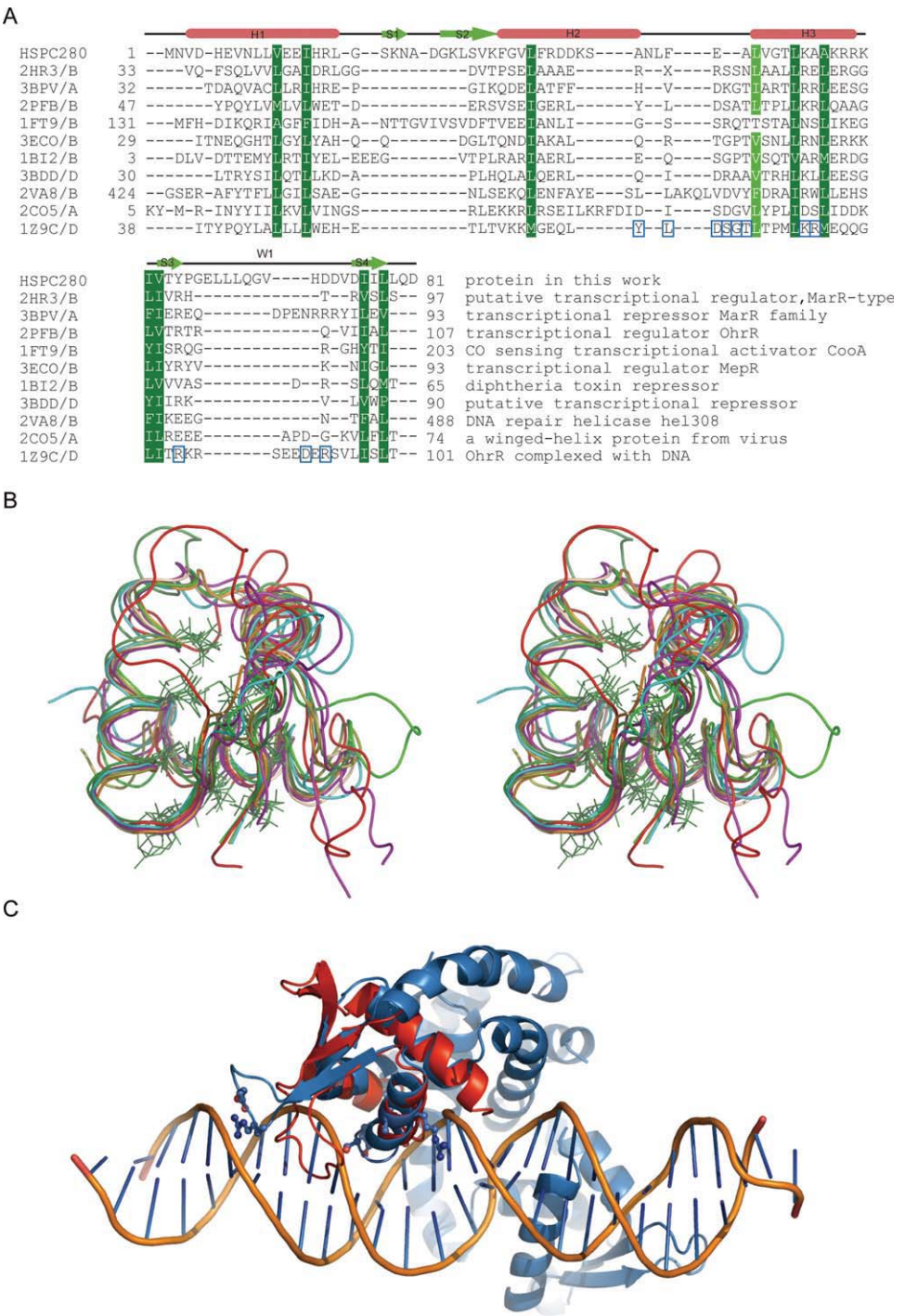

Figure 2. A: Structure based multiple sequence alignment of structural homologs of HSPC280. Sequences are arranged in the order of *z*-scores and named by PDB accession number and chain. Each sequence is followed by a short description of the proteins. The secondary structural elements are indicated above, based on the HSPC280 structure. Conserved residues are shaded in green. The key residues involved in DNA binding for the last sequence (PDB 1Z9C), and protein OhrR bound with DNA, are boxed in blue. B: Stereo view of the structural superimposition of these proteins. The side-chains of the conserved residues indicated in (A) are shown as green lines. C: Structural superimposition of HSPC280 (red) and OhrR (blue) bound with DNA. The key residues in OhrR involved in DNA binding as indicated in (A) are shown as sticks.

To detect whether HSPC280 interacts with DNA, we obtained 2D ^{1}H-^{15}N HSQC spectra for HSPC280 in the presence and absence of DNA at pH 7.0 and 4.4. The 2D ^{1}H-^{15}N HSQC spectra of HSPC280 with and without DNA obtained at pH 7.0 and 4.4 showed no explicit signal shifting (Supporting Information Fig. S3), suggesting that HSPC280 cannot interact with DNA. However, specific/nonspecific interactions with DNA have been detected for most winged-helix proteins at pH $>$ 7.0. It is likely that the negatively and positively polarized electrostatic surfaces [Fig. 1(D)] may influence the

interaction between HSPC280 and DNA, since the charge characteristics of the protein surface affect the electrostatic interaction with the ribose-phosphate backbone of DNA. In addition, to test whether HSPC280 binds to nucleic acids *in vitro*, an EMSA was carried out with recombinant HSPC280 using single and double-stranded DNA and RNA. However, no significant binding of HSPC280 to DNA or RNA could be detected. Therefore, HSPC280 is not a typical DNA-binding winged-helix protein.

Interestingly, a sequence search revealed a protein family named Abra (also known as Stars) whose C-terminal portion (last 80 residues) shows 30% protein sequence identity with HSPC280 [Fig. 1(A)], suggesting that the C-terminal portion of Abra can fold into a single HSPC280-like domain. Abra is a muscle-specific actin-binding protein capable of stimulating SRF-dependent transcription by a mechanism involving RhoA and actin polymerization[26] and is also involved in human skeletal muscle hypertrophy and atrophy.[27] It might be essential for fluid shear stress-induced arteriogenesis.[28] As is well known, human Abra is a protein of 384 amino acids and its C-terminal 142 residues are responsible for F-actin binding. Deletion of the last 80 residues of Abra abolishes its F-actin binding ability.[26] It seems the winged-helix domain of Abra should thus be involved in the F-actin binding ability. Based on this information, we performed an *in vitro* F-actin binding assay for HSPC280 and failed to detect such a binding event (Supporting Information Fig. S4). Nevertheless, many hydrophobic residues are conserved between HSPC280 and the Abra (last 80 residues) family [Fig. 1(A)]. Some of the conserved hydrophobic residues (V7, L10, I14, G31, L33, L50, and A53) of HSPC280 are involved in hydrophobic interactions inside the winged-helix structural core, and some other hydrophobic conserved residues are clustered on the surface of the protein. Conserved residues F30 and F34 in helix α2 and residues L46, V47, and G48 in helix α3 are clustered together with conserved residues L65, L66, and L67 in wing 1 on the protein surface forming a hydrophobic surface patch coincident with the groove between wing 1 and helices α3 and α2, possibly allowing HSPC280 to interact with other proteins. In addition, the conserved hydrophilic residues, K54 and R55 from helix α3 and E64 in wing 1 form a hydrophilic surface patch which is located on the side where the hydrophobic conserved patch is located on the protein [Fig. 1(E)]. These conserved surface patches may serve as sites for the interaction of HSPC280 with other proteins and may have some functional role.

Materials and Methods

Protein expression and purification

The C6ORF115 gene was amplified from a human liver cDNA library and cloned into the pET-22a expression vector between the NdeI and XhoI restriction sites. The resulting construct contained eight additional residues at the C-terminus (LEHHHHHHH) that facilitate protein purification. Uniformly ^{15}N- and $^{15}N/^{13}C$-labeled HSPC280 was produced in the BL21(DE3) *E.coli* strain in M9 minimal medium containing $^{15}NH_4Cl$ and [^{13}C]-glucose as the sole nitrogen and carbon sources, respectively. Cells were grown at 37°C until an OD_{600} of 0.7 and then induced with 1 m*M* isopropyl-β-D-thiogalactopyranoside (IPTG) for 3 h at 37°C. The protein was then purified on a metal chelating column (GE healthcare) followed by gel filtration (Sephedex G50). The purified protein was dialyzed against distilled water or 100 m*M* NH_4HCO_3 and then lyophilized and stored at −80°C.

The recombinant HSPC280 was not stable during NMR data collection, possibly because of the existence of a cysteine residue (Cys39) which may be exposed to solvent. To obtain high quality NMR spectra, the cysteine at sequence position 39 was replaced by serine. The C39S-mutant HSPC280 ([C39S]HSPC280) was purified in the same manner as native HSPC280. The 2D ^{1}H-^{15}N HSQC spectrum of [C39S]HSPC280 was essentially the same as that for the native protein, suggesting that the mutation of a single amino acid did not influence the overall structure of HSPC280. Samples of [C39S]HSPC280 were used in this study; [C39S]HSPC280 is referred to as HSPC280 throughout the text. Protein purity was assessed by SDS-PAGE and was shown to be a single band.

NMR spectroscopy

Samples were prepared by dissolving 2 m*M* HSPC280 in 90% H_2O/10% D_2O containing 20 m*M* deuterated acetate buffer (pH 4.4) and 20 m*M* KCl. 2D and 3D heteronuclear NMR experiments were performed at 310 K on a Bruker DMX600 spectrometer equipped with a z-gradient triple-resonance cryo-probe. All NMR data obtained were processed with FELIX98 (Accelrys Inc.) and analyzed with SPARKY. Backbone resonance assignments were derived from 2D ^{1}H-^{15}N HSQC and 3D ^{1}H-^{13}C-^{15}N HNCA, HNCACB, CBCA(CO)NH, HNCO, and HN(CA)CO experiments, and the program AutoAssign[29] was used to assist the assignments. Side-chain resonance assignments were obtained from 3D HBHA(CBCA)CONH, HBHA(CBCA)NH, and (H)CCH-TOCSY spectra. The 3D ^{1}H-^{15}N NOESY-HSQC experiment (τ_m = 180 ms) and 3D ^{1}H-^{13}C NOESY-HSQC experiments for aliphatic and aromatic regions were carried out using a mixing time of 150 ms to obtain the NOE distance constraints. Proton chemical shifts were calibrated relative to internal 0.25 m*M* DSS (2,2-dimethyl-2-silapentane-5-sulfonate). ^{15}N and ^{13}C chemical shifts were referenced indirectly.

The relaxation parameters, ^{15}N R_1 and R_2 and ^{1}H–^{15}N NOE, were measured for 1.0 m*M* ^{15}N-labeled HSPC280 in buffer (20 m*M* NaAc/DAc, 100 m*M* KCl, pH 4.4) at 310 K using standard methods.[30] For ^{15}N R_1 measurements, delay times were set to 20 × 2, 40, 80, 160, 250, 400, 650, 1000, and 1500 ms. For ^{15}N R_2 measurements, relaxation delays were set to 16.96×2, 33.92, 50.88, 67.84, 84.80, 101.76, 118.72, 135.68, 169.60, 220.48, 254.40, and 305.28 ms. In the 2D ^{1}H–^{15}N NOE experiments, a delay of 6 s was followed by ^{1}H saturation for 3 s, while the saturation period was replaced by a delay of 9 s in the control experiment. The two experiments were run in an interleaved manner. The NOE values were calculated from the ratios of the peak intensities with and without proton saturation. R_1 and R_2 relaxation rates were determined by fitting peak intensities of the spectra acquired at various relaxation delay times to an exponential decay function, $I/I_0 = \exp(-R_{1,2}t)$, where I_0 is the intensity at $t = 0$ and I is the intensity after a time delay t.

To explore the interactions between HSPC280 and DNA, a new construct in which the His-tag was removed was obtained. 2D ^{1}H-^{15}N HSQC experiments were performed on HSPC280 without the His-tag in the absence and presence of DNA at pH 4.4 and pH 7.0. The 2D ^{1}H-^{15}N HSQC spectra of 0.1 m*M* ^{15}N-labeled HSPC280 dissolved in 50 m*M* DAc/NaAc (pH 4.4) or 50 m*M* phosphate (pH 7.0) buffer containing 200 m*M* KCl in the absence of DNA and in the presence of DNA at protein/DNA molar ratios of 1:0.5 and 1:3.0 were acquired. A 10-bp duplex DNA containing GCGAATTCGC was used in the experiments.

Structure calculation

The initial structure of HSPC280 was generated using the CANDID module of CYANA.[31] NOE assignments from CANDID were checked manually. Hundred and thirty seven backbone dihedral angle restraints obtained from chemical shift data using the program TALOS[32] were used in the initial structure calculation. Sixty four hydrogen bond restraints were introduced in later rounds of structure calculations. Of a family of 100 structures generated in the final round, the 40 lowest-energy structures were refined in explicit water using xplor-nih,[33] from which the 20 lowest-energy structures were selected for final analysis. The quality of the structure ensemble was validated using the program PROCHECK-NMR.[34]

Coordinates

The atomic coordinates of the HSPC280 structure have been deposited in the Protein Data Bank under ID code 212O.

Conclusions

The solution structure of HSPC280 has a winged helix-like fold showing positively and negatively charged surfaces on the two sides of the protein structure. HSPC280 is not a genuine winged-helix protein. Unlike most winged-helix proteins and domains which show specific/nonspecific binding with DNA at pH 7.0, HSPC280 cannot interact with DNA. The presence of a hydrophobic surface patch that is conserved between HSPC280 and proteins in the Abra family implies that HSPC280 might be involved in protein–protein interactions and play a significant functional role.

References

1. Molina H, Bunkenborg J, Reddy GH, Muthusamy B, Scheel PJ, Pandey A (2005) A proteomic analysis of human hemodialysis fluid. Mol Cell Proteomics 4: 637–650.
2. Chan K, Lucas D, Hise D, Schaefer C, Xiao Z, Janini G, Buetow K, Issaq H, Veenstra T, Conrads T (2004) Analysis of the human serum proteome. Clin Proteomics 1:101–225.
3. Wasinger VC, Locke VL, Raftery MJ, Larance M, Rothemund D, Liew A, Bate I, Guilhaus M (2005) Two-dimensional liquid chromatography/tandem mass spectrometry analysis of Gradiflow fractionated native human plasma. Proteomics 5:3397–3401.
4. Hardwidge PR, Rodriguez-EscuderoI, Goode D, Donohoe S, Eng J, Goodlett DR, Aebersold R, Finlay BB (2004) Proteomic analysis of the intestinal epithelial cell response to enteropathogenic *Escherichia coli*. J Biol Chem 279:20127–20136.
5. Lambrecht S, Dhaenens M, Almqvist F, Verdonk P, Verbruggen G, Deforce D, Elewaut D (2009) Proteome characterization of human articular chondrocytes leads to novel insights in the function of small heat-shock proteins in chondrocyte homeostasis. Osteoarthritis Cartilage 18:440–446.
6. Greening DW, Glenister KM, Kapp EA, Moritz RL, Sparrow RL, Lynch GW, Simpson RJ (2008) Comparison of human platelet membrane-cytoskeletal proteins with the plasma proteome: towards understanding the platelet-plasma nexus. Proteomics Clin Appl 2:63–77.
7. Yan W, Lee H, Yi EC, Reiss D, Shannon P, Kwieciszewski BK, Coito C, Li XJ, Keller A, Eng J, Galitski T, Goodlett DR, Aebersold R, Katze MG (2004) System-based proteomic analysis of the interferon response in human liver cells. Genome Biol 5:R54.
8. van der Heul-Nieuwenhuijsen L, Hendriksen PJ, van der Kwast TH, Jenster G (2006) Gene expression profiling of the human prostate zones. BJU Int 98:886–897.
9. Wang IM, Stepaniants S, Boie Y, Mortimer JR, Kennedy B, Elliott M, Hayashi S, Loy L, Coulter S, Cervino S, Harris J, Thornton M, Raubertas R, Roberts C, Hogg JC, Crackower M, O'Neill G, Pare PD (2008) Gene expression profiling in patients with chronic obstructive pulmonary disease and lung cancer. Am J Respir Crit Care Med 177:402–411.
10. Gevaert K, Goethals M, Martens L, Van Damme J, Staes A, Thomas GR, Vandekerckhove J (2003) Exploring proteomes and analyzing protein processing by mass spectrometric identification of sorted N-terminal peptides. Nat Biotechnol 21:566–569.
11. Jinawath N, Furukawa Y, Hasegawa S, Li M, Tsunoda T, Satoh S, Yamaguchi T, Imamura H, Inoue M,

Shiozaki H, Nakamura Y (2004) Comparison of gene-expression profiles between diffuse- and intestinal-type gastric cancers using a genome-wide cDNA microarray. Oncogene 23:6830–6844.
12. Caffarel MM, Moreno-Bueno G, Cerutti C, Palacios J, Guzman M, Mechta-Grigoriou F, Sanchez C (2008) JunD is involved in the antiproliferative effect of Delta9-tetrahydrocannabinol on human breast cancer cells. Oncogene 27:5033–5044.
13. Vuister GW, Kim SJ, Orosz A, Marquardt J, Wu C, Bax A (1994) Solution structure of the DNA-binding domain of Drosophila heat shock transcription factor. Nat Struct Biol 1:605–614.
14. Damberger FF, Pelton JG, Harrison CJ, Nelson HC, Wemmer DE (1994) Solution structure of the DNA-binding domain of the heat shock transcription factor determined by multidimensional heteronuclear magnetic resonance spectroscopy. Protein Sci 3:1806–1821.
15. Meinhart A, Blobel J, Cramer P (2003) An extended winged helix domain in general transcription factor E/IIE alpha. J Biol Chem 278:48267–48274.
16. Holm L, Rosenstrom P (2010) Dali server: conservation mapping in 3D. Nucleic Acids Res 38 Suppl:W545–W549.
17. Hong M, Fuangthong M, Helmann JD, Brennan RG (2005) Structure of an OhrR-ohrA operator complex reveals the DNA binding mechanism of the MarR family. Mol Cell 20:131–141.
18. Clark KL, Halay ED, Lai E, Burley SK (1993) Co-crystal structure of the HNF-3/fork head DNA-recognition motif resembles histone H5. Nature 364:412–420.
19. Zheng N, Fraenkel E, Pabo CO, Pavletich NP (1999) Structural basis of DNA recognition by the heterodimeric cell cycle transcription factor E2F-DP. Genes Dev 13:666–674.
20. Jin C, Marsden I, Chen X, Liao X (1999) Dynamic DNA contacts observed in the NMR structure of winged helix protein-DNA complex. J Mol Biol 289: 683–690.
21. van Dongen MJ, Cederberg A, Carlsson P, Enerback S, Wikstrom M (2000) Solution structure and dynamics of the DNA-binding domain of the adipocyte-transcription factor FREAC-11. J Mol Biol 296:351–359.
22. Gajiwala KS, Chen H, Cornille F, Roques BP, Reith W, Mach B, Burley SK (2000) Structure of the winged-helix protein hRFX1 reveals a new mode of DNA binding. Nature 403:916–921.
23. Overdier DG, Porcella A, Costa RH (1994) The DNA-binding specificity of the hepatocyte nuclear factor 3/forkhead domain is influenced by amino-acid residues adjacent to the recognition helix. Mol Cell Biol 14: 2755–2766.
24. Shiyanova T, Liao X (1999) The dissociation rate of a winged helix protein-DNA complex is influenced by non-DNA contact residues. Arch Biochem Biophys 362: 356–362.
25. Weigelt J, Climent I, Dahlman-Wright K, Wikstrom M (2001) Solution structure of the DNA binding domain of the human forkhead transcription factor AFX (FOXO4). Biochemistry 40:5861–5869.
26. Arai A, Spencer JA, Olson EN (2002) STARS, a striated muscle activator of Rho signaling and serum response factor-dependen ttranscription. J Biol Chem 277: 24453–24459.
27. Lamon S, Wallace MA, Leger B, Russell AP (2009) Regulation of STARS and its downstream targets suggest a novel pathway involved in human skeletal muscle hypertrophy and atrophy. J Physiol 587:1795–1803.
28. Troidl K, Ruding I, Cai WJ, Mucke Y, Grossekettler L, Piotrowska I, Apfelbeck H, Schierling W, Volger OL, Horrevoets AJ, Grote K, Schmitz-Rixen T, Schaper W, Troidl C (2009) Actin-binding rho activating protein (Abra) is essential for fluid shear stress-induced arteriogenesis. Arterioscler Thromb Vasc Biol 29: 2093–2101.
29. Moseley HN, Monleon D, Montelione GT (2001) Automatic determination of protein backbone resonance assignments from triple resonance nuclear magnetic resonance data. Methods Enzymol 339:91–108.
30. Farrow NA, Muhandiram R, Singer AU, Pascal SM, Kay CM, Gish G, Shoelson SE, Pawson T, Forman-Kay JD, KayLE (1994) Backbone dynamics of a free and phosphopeptide-complexed Src homology 2 domain studied by ^{15}N NMR relaxation. Biochemistry 33: 5984–6003.
31. Guntert P (2004) Automated NMR structure calculation with CYANA. Methods Mol Biol 278:353–378.
32. Cornilescu G, Delaglio F, Bax A (1999) Protein backbone angle restraints from searching a database for chemical shift and sequence homology. J Biomol NMR 13:289–302.
33. Schwieters CD, Kuszewski JJ, Tjandra N, Clore GM (2003) The Xplor-NIH NMR molecular structure determination package. J Magn Reson 160:65–73.
34. Laskowski RA, Rullmannn JA, MacArthur MW, Kaptein R, Thornton JM (1996) AQUA and PROCHECK-NMR: programs for checking the quality of protein structures solved by NMR. J Biomol NMR 8:477–486.